JES Focus Issue on Processes at the Semiconductor-Solution Interface

Olivine-$LiNiPO_4$ Thin Films: Chemical Compatibility with Liquid Electrolyte and Interface Stability at High Potential

Gennady Cherkashinin,[1,z] Robert Eilhardt,[1] Mikhail V. Lebedev,[2] Silvia Nappini,[3] Elena Magnano,[3,4] and Wolfram Jaegermann[1]

[1]*Institute of Materials Science, Technische Universität Darmstadt, D-64287 Darmstadt, Germany*
[2]*Ioffe Institute, St. Petersburg 194021, Russia*
[3]*IOM CNR Laboratorio TASC, 34149 Basovizza, Trieste, Italy*
[4]*Department of Physics, University of Johannesburg, 2006 Johannesburg, South Africa*

The chemical compatibility between carbon free olivine-$LiNiPO_4$ thin films used as cathode material and $LiPF_6$/DMC/FEC/0.2%-TMB liquid electrolyte was studied by soft-photoelectron spectroscopy, Ni L- and O K- XANES combined with electrochemical experiments. The stability of the electrolyte-electrode interface at a high charging potential strongly depends on the temperature of $LiNiPO_4$ preparation. For the films grown at 740°C, the chemical composition of the interface is not changed even at a charging potential of 5.2 V, whereas the electrolyte-electrode interface of $LiNiPO_4$ grown at lower temperatures (675°C) decomposes at 5.1 V, involving the cathode material in the chemical reaction.

 [DOI: 10.1149/2.0211804jes]

Manuscript submitted October 24, 2017; revised manuscript received January 15, 2018. Published January 30, 2018. *This paper is part of the JES Focus Issue on Processes at the Semiconductor-Solution Interface.*

The development of high energy density as well as high power density devices for plug-in hybrid electric vehicles is still a challenge, which demands the fundamental understanding of the thermodynamic stability range of redox active materials and physicochemical properties of the electrode-electrolyte interface. Spontaneous altering of the electronic structure of the electrode materials and chemical composition at the electrolyte-electrode interface under a charging potential impacts the Li^+ ions transport across the interface, thereby significantly reducing the power supplied by the battery cell and leading to its fast degradation.[1] Olivine-$LiMPO_4$ (M = Co, Ni) provides a high redox potential (~5 V vs Li/Li^+) due to a favorable electronic configuration of the M^{2+}(3d) and PO_4^{3-} states, giving a theoretical energy density of ~850 Wh kg^{-1} of the olivine-based battery cell. However, such a high potential dictates to use electrolytes, which are stable in the wide voltage window (VW) range. In spite of progress in the development of highly conductive ionic liquids or solid electrolytes (VW > 5 V),[2,3] the organic liquid electrolytes still have the highest ionic conductivity, although their stability range does not exceed 5 V.[4]

Here, we explore the chemical compatibility of carbon-free olivine-$LiNiPO_4$ (LNP) thin film material with $LiPF_6$/DMC/FEC/0.2%-TMB liquid electrolyte in dependence on temperature of the thin film growth. Quasi in-situ soft photoelectron spectroscopy (SPES) and X-ray absorption near edge spectroscopy (XANES) combined with electrochemical experiments are used to study the evolution of the electronic structure at the Fermi level (E_F), oxidation and spin state, as well as the chemical composition at the electrode-electrolyte interface formed by the emersion at various charging potentials.

Experimental

Quasi in-situ synchrotron photoelectron emission experiments on LNP thin films grown under different conditions combined with the electrochemical experiments were carried out at BESSY II (Berlin). The pristine LNP films were in addition studied by using synchrotron facilities at Elettra (Trieste). The SPES, Ni L- and O K- XANES were performed at the U56-2/PGM-1 undulator beamline using the Solid Liquid Interface Analysis (SoLiAS) endstation equipped with a SPECS PHOIBOS 150 MCD-9 electron analyzer. In Elettra, the SPES and XANES experiments were carried out on BACH elliptically polarized undulator beamline. The BACH endstation is equipped with VG-Scienta R3000 hemispherical analyser. The binding energies were referenced to the E_F of a clean Ag foil. The polycrystalline olivine-LNP thin films were deposited on a Pt foil by using radio-frequency sputtering of a $LiNiPO_4$ target material at room temperature in argon-oxygen atmosphere ($p \approx 1 \times 10^{-2}$ mbar) followed by annealing in air at different temperatures. The deposition setup is reported elsewhere.[5,6] After the photoemission experiments, a pristine-LNP film was transported in Ar-atmosphere to a glovebox (MBRAUN GmbH). The electrochemical charging of LNP films was carried out in the 3.1–5.2 V range (Gamry Instrument, Interface 1000 TM) by using a Swagelok-type two electrode cell. 1 M $LiPF_6$ in 4:1 wt/wt Dimethyl Carbonate (DMC): Fluorinated Ethylene Carbonate (FEC) + 0.2%wt Trimethylboroxine (TMB) (Solvionic) was used as an electrolyte. A lithium foil was used as anode and Celgard 2500 as separator. The current vs time characteristics were recorded until reaching a steady state under a certain charging potential. The holding time for each charging potential was ~30 min (Fig. 1S, Supplementary Material). The cell was then disassembled, the LNP film was rinsed in DMC, dried in Ar-atmosphere and transported under argon to SoLiAS for further photoemission and XANES experiments.

Results and Discussion

Figures 1a, 1b show the Ni L- and O K- XANES of pristine LNP thin film and their evolution under a charging potential. The shape of the Ni L edge evidences the existence of $Ni^{2+}(t_{2g}{}^3\uparrow t_{2g}{}^3\downarrow e_g{}^2\uparrow)$ ions. The O K edge, Fig. 1b, is typical for orthophosphate PO_4^{3-} with the broad feature *A* ascribed to the transition from O1s core level to the empty O2p orbital hybridized with the p orbitals of phosphor.[7] The pre-edge peak *B*, Fig. 1b, is inherent to olivine-$LiMPO_4$ compounds and ascribed to the unoccupied M3d-O2p hybridized states.[8–10] The spectral features of the valence band (VB) spectra, Fig. 1e, near the VB maximum, E_{VBM}, are associated with the strongly hybridizied Ni3d-O2p states, whereas the VB emission at higher energies is attributed to strongly bound phosphorus and oxygen states.

Intact shape of the core-level photoemission and X-ray absorption spectra after contact of the films to the electrolyte, Figs. 1aii–1dii, evidence the stability of the cathode material showing invariability of its electronic configuration at open circuit voltage (OCV) conditions. An enhanced VB emission in the 8–14 eV binding energy range, Fig. 1eii, is attributed to the carbon groups and F- containing species of the electrolyte adsorbed on the LNP surface (see the

[z]E-mail: cherk@surface.tu-darmstadt.de

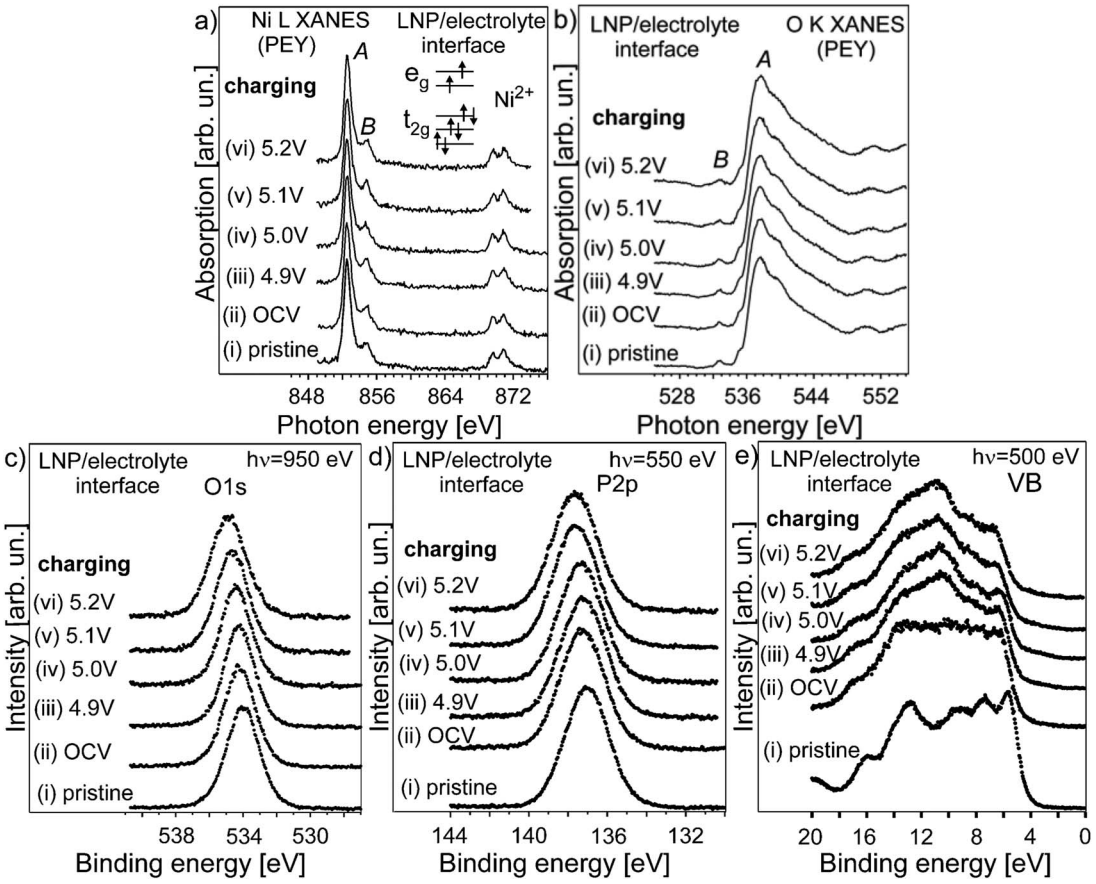

Figure 1. Ni L- (a), O K- (b) XANES, O1s- (c), P2p- (d) and VB- (e) photoelectron emissions of a $LiNiPO_4$ thin film (T = 740°C) contacted to the $LiPF_6$/DMC/FEC/0.2%-TMB electrolyte vs the charging potential. OCV is open circuit voltage. The analysis depth is d∼50 Å. PEY is the partial electron yield mode.

discussion on the core level photoemissions below). Various carbonate solvents exhibit spectral features at 2–4 eV from E_{VBM} as shown for the electrolyte-$LiCoO_2$ interfaces,[11] whereas the F2p orbital of LiF is situated at ∼2 eV from E_{VBM}.[12] The contact of LNP films to the liquid electrolyte leads also to a slight E_F shift (∼0.2 eV) away from the E_{VBM}, Fig. 2a. The downward band bending was revealed for various ionic conductor- liquid interfaces; the different charge transfer mechanisms were widely discussed in the past.[11,13,14] The solid electrolyte interface (SEI), Figs. 2b, 2c, is composed of FEC- and $LiPF_6$- based species, among which C-O, -(CH_2-CH_2-O)-, CO-C(O) = C, C-F, LiF, Li_xPF_y and $Li_xPO_yF_z$ are probable decomposition products.[15–17] The possible shift of the core-levels of LNP to higher binding energies complicates the unambiguous assignment of the relevant species. However, since the O1s photoelectron emission is not markedly changed, Fig. 1c, we assume that the SEI layer includes a high percentage of alkyl carbon, as well as the decarboxylation products associated with the reduction of FEC.[17,18] The predominance of oxygen-free organic species over oxygen-containing organic

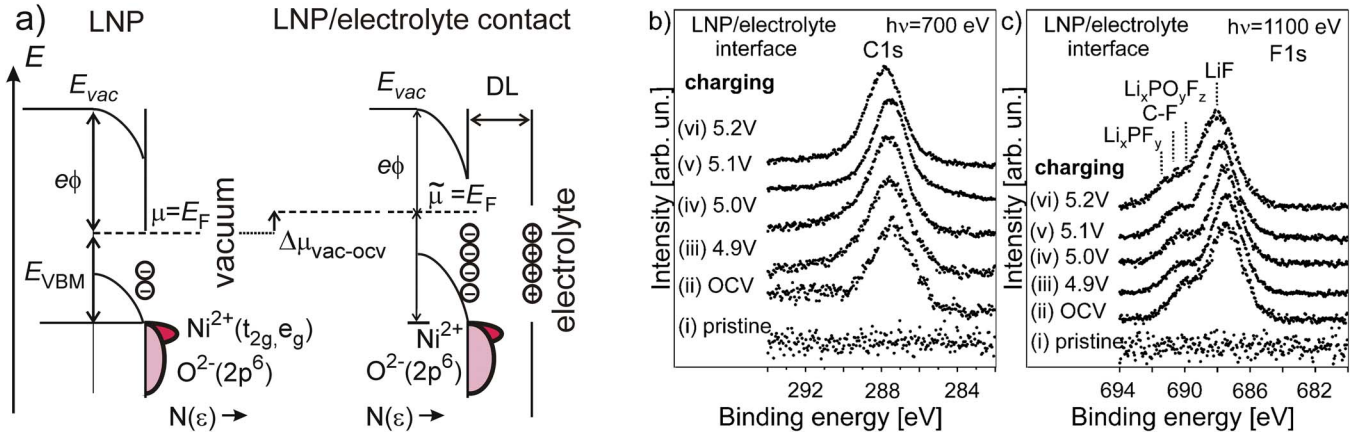

Figure 2. Energy band diagram (a) of a $LiNiPO_4$ thin film (T = 740°C) contacted to the $LiPF_6$/DMC/FEC/0.2%-TMB electrolyte (a), C1s- (b), F1s– (c) photoelectron emissions vs the charging potential. DL is double layer on electrolyte side (a). E_{VBM} is the valence band maximum. The Ni^{2+} ions remain at the interface (a). The analysis depth is d∼50 Å.

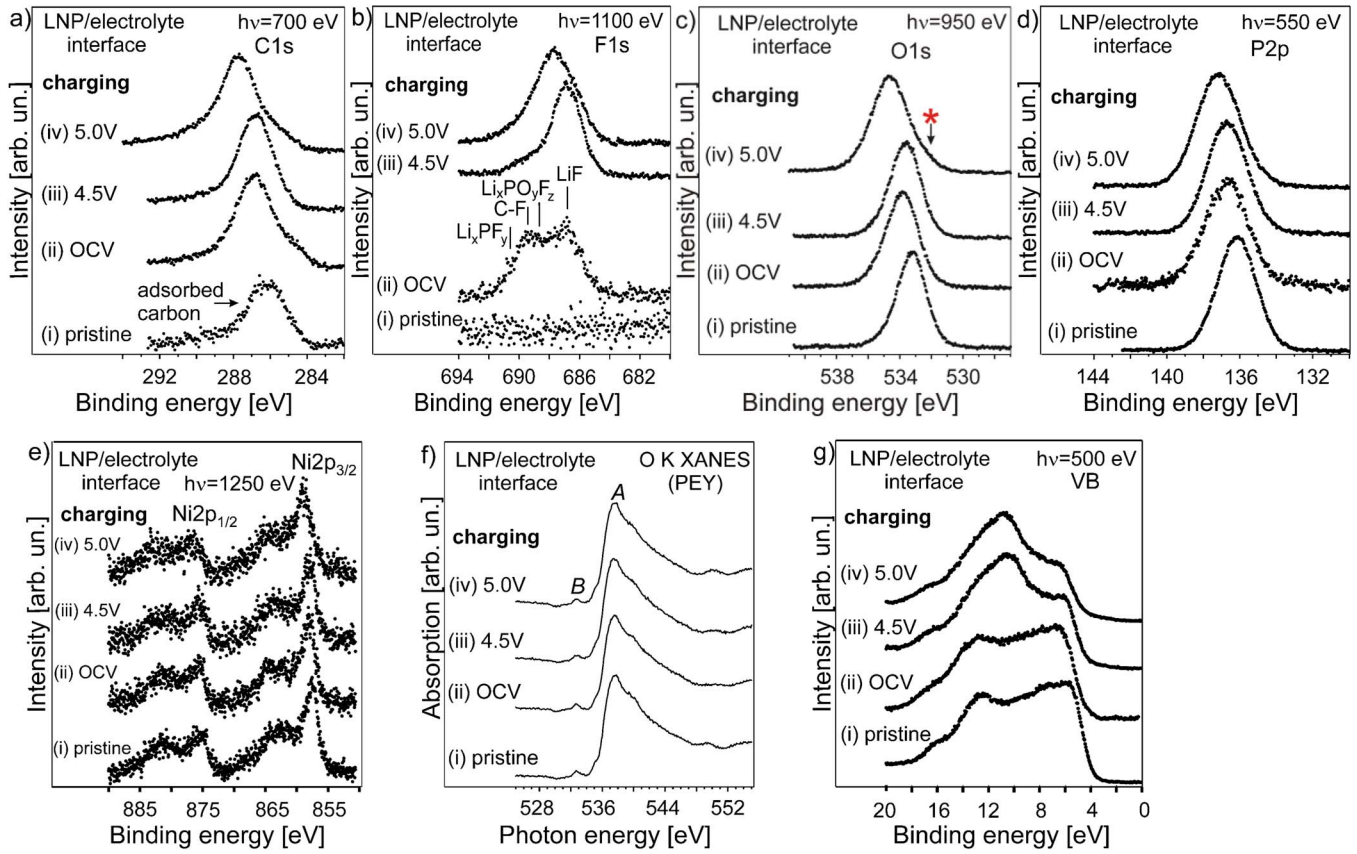

Figure 3. C1s- (a), F 1s- (b), O1s- (c), P2p- (d), Ni2p- (e) photoelectron emissions and O K XANES (f) of a $LiNiPO_4$ thin film (T = 700°C) in contact with the $LiPF_6$/DMC/FEC/0.2%-TMB electrolyte vs the charging potential. OCV is open circuit voltage. The pristine LNP film was stored under high vacuum conditions ($p \sim 10^{-8}$ mbar) for ∼1 week. The analysis depth is d∼50 Å. The background of the Ni2p photoelectron spectra is removed by using the Shirley approach. The beginning of the decomposition of the SEI layer is shown by a star (*). PEY is the partial electron yield mode.

polymers, alkoxides and carbonates, as well as LiF over other F-containing species (Fig. 2c) was also observed at the surface reactions of FEC on Si-anode materials, where the formation of the unsaturated polymer compounds from the reduction of FEC was presumed.[17,19]

Under the charging potential, the SEI chemical composition is not changed significantly, Figs. 2b, 2c, thereby evidencing no further decomposition of the electrolyte. The chemical reactions with the surface of LNP thin film electrode will not take place even at the charging potential of 5.2 V. The invariance of the Ni and oxygen oxidation states, as well as the shift of the core-levels and VB structure away from the E_F after the charging potential application does not suggest any charge transfer to the metal or anion sites of LNP, which would be a sign of a delithiation process. One should note that the charge compensation demands the valence electron withdrawal from the host material accompanied by the shift of the E_F to the E_{VBM}.[13] The studies of the electron structure agree with cyclic voltammograms of the LNP thin films, which do not exhibit redox peaks (Figure 2S, Supplementary Material). The expected oxidation of LNP cathode material occurs at the 5.18 V–5.3 V range, whereas the reduction takes place at 4.9 V–5.1 V.[20,21] However, electronic conductivity has to be sufficiently high to activate the redox process. The voltage profile of the LNP/C composite cathode material (84% LNP, 8% carbon black and 8% binder) does not exhibit the well resolved oxidation/reduction peaks,[21] if the conductive surface coating or the lattice doping, enhancing significantly the electrode reaction reversibility, are not used.[22] Our recent study on $LiCoPO_4$ (LCP) carbon-free thin films has demonstrated an important role of the surface morphology for providing high electronic and Li-ion conductivity of the cathode material. The surface area of the LNP thin films is not large as compared to electrochemically active LCP (Fig. 3S, Supplementary Material), being an additional argument of insufficient electronic conductivity of the LNP thin film material.

The stability of the SEI layer strongly depends on the growth conditions of the LNP films. The evolution of the electronic structure at the electrode-electrolyte interface for the LNP film grown at T = 700°C and T = 675°C is shown in Figs. 3a–3g and 4a–4g, respectively. The shift of the photoelectron spectra to lower binding energies (Figs. 3ci, 3di, 4ci, 3di), as compared to the LNP film prepared at higher temperature (Fig. 1ci, 1di), is explained by higher conductivity, as well as by a decrease in the Ni3d-O2p hybridization strength of LNPs annealed at lower temperatures. Similar to the film grown at T = 740°C, the contact of LNPs to electrolyte does not lead either to changes of the oxidation states of divalent Ni ions and PO_4^{3-} polyanion or in the chemical composition at the interfaces, Figs. 3a–3g, 4a–4g. Some differences in the shape of the F1s photoemission spectra are observed for LNP (T = 700°C). In particular, the ratio between the intensities of LiF and other F- related species is different, as compared to the films annealed at 675°C and 740°C (Figs. 2cii, 3bii, 4bii). Besides, in spite of the similarity in the chemical composition for all three LNP-interfaces, the intensities of the F- related and carbon species are correlated as follows: the higher carbon content, the lower content of F-related species (675°C) and, vice versa, the much lower carbon content, the higher content of F- species (740°C). The stability of the SEI layer is preserved up to a charging potential of 4.8 V independently of the preparation temperature of the LNP films. The first signs of the LNP-electrolyte interface decomposition occur at 5.0 V for the LNP annealed at the intermediated temperature (T = 700°C), Fig. 3. It is accompanied by a broadening of the O1s and P2p photoemissions (Figs. 3c, 3d) although the changes in the relative content of the F-containing species take place at 4.5 V (Fig. 3b).

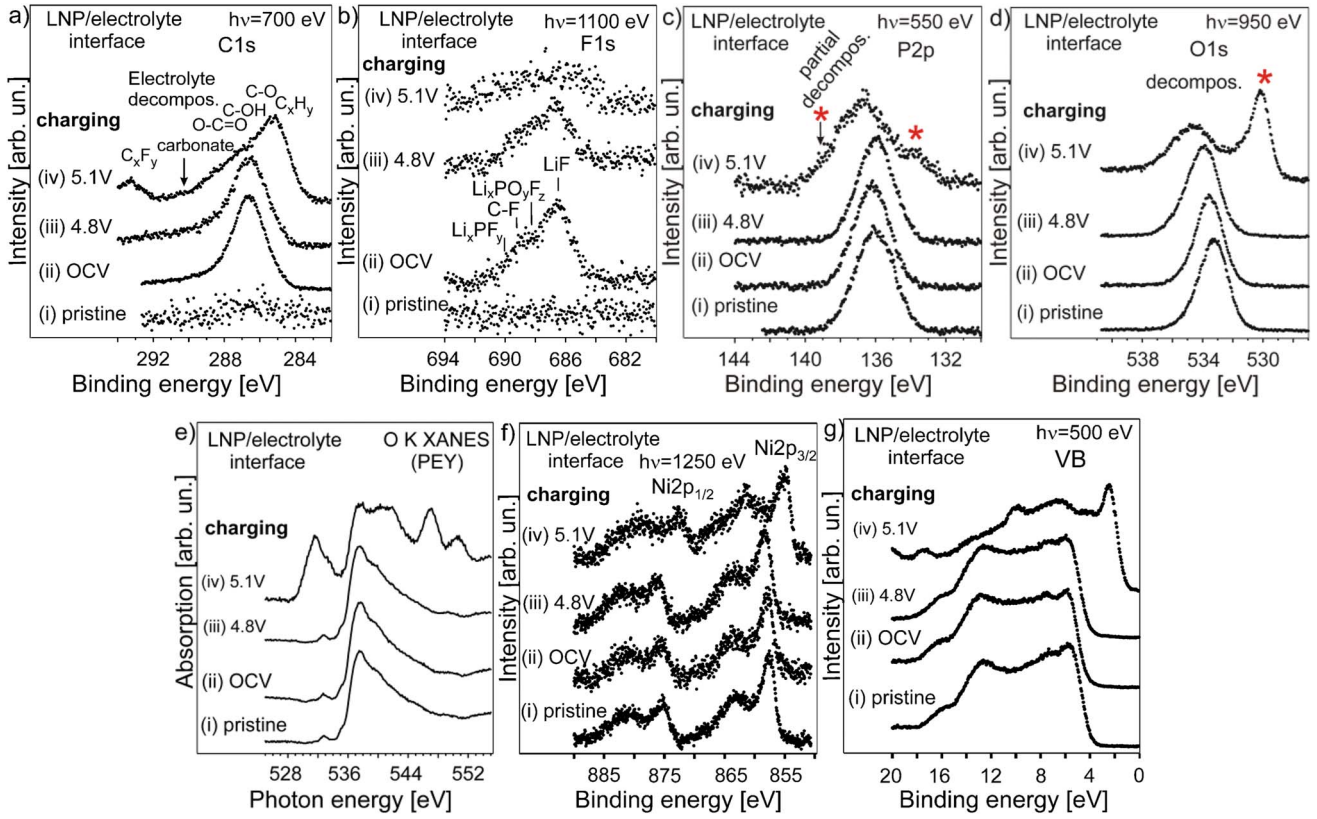

Figure 4. C1s- (a), F 1s- (b), P2p- (c), O1s- (d) photoelectron emissions, O K XANES (e), Ni2p- (f) and VB- (g) photoelectron emissions of a $LiNiPO_4$ thin film (T = 675°C) in contact with the $LiPF_6$/DMC/FEC/0.2%-TMB electrolyte vs the charging potential. OCV is open circuit voltage. The analysis depth is d∼50 Å. The background of the Ni2p photoelectron spectra is removed by using the Shirley approach. The decomposition of the SEI layer is shown by a star (*). PEY is the partial electron yield mode.

However, severe changes in the electronic structure and chemical composition are revealed in the LNP film grown at the lowest temperature (T = 675°C), Figs. 4aiv–4giv. Under a charging potential of 5.1 V, the decomposition of the SEI layer is accompanied by the formation of additional carbon species, depletion of the F-related species and the involvement of LNP in the chemical reaction, Figs. 4aiv–4giv. SEI dissolution accompanied by Co^{3+} ion reduction was already observed in the NMC layered cathode material charged to a high potential, which was explained by the lattice expansion followed by the weakening and breaking of the chemical bonds of organic molecules constituting the SEI layer.[23] One plausible reason for the different sustainability of the LNP-electrolyte interfaces at a high potential is assigned to the surface defects of the pristine LNPs, the amount of which, as well as their nature are defined by the film preparation conditions. Among possible non-stoichiometric phases in olivine-LNP films grown at lower temperatures are the inclusions of amorphous phase or/and phosphor-oxygen groups, which do not belong to the olivine structure. The pristine LNP film grown at 740°C exhibits well resolved spectral features in the VB spectrum, Fig. 1ei, thereby evidencing a well ordered structure. On the other hand, the spectral features of the LNP films grown at lower temperatures are rather smooth, Figs. 3gi, 4gi, due to overlapping of the valence levels of olivine and non-stoichiometric surface phases, which are probably responsible for leveling the spectral feature at ∼10 eV from E_F (the latter is well visible in LNP film grown at 740°C, see Fig. 1e and Figs. 3g, 4g for comparison). For a more detailed analysis, DFT calculations of the density of occupied states near E_F are necessary. Although the coating with phosphates is often used as a protective layer in the layered cathode materials,[24] the performance of these battery cells is usually studied in the voltage range below 5.0 V, where the SEI layer is stable for all studied LNP films (Figs. 1–4). The issue of the decreased life cycle of the olivine based battery cells due the secondary phases dissolution in electrolytes has been recently raised.[25] Non-stoichiometric composition at the surface can promote the chemical reactions with the adsorbed electrolyte under a high potential, resulting in the destabilization of the interface followed by its dissolution and the formation of a volatile phase evaporated under vacuum conditions. The obtained results evidence that the SEI layer with a higher content of the F-related species, formed under adsorption of the electrolyte and under a charging potential, protects the buried LNP more efficiently (Figs. 2c, 3b, 4b). However, the mechanism is not clear yet and demands further investigations. As the thin SEI cannot protect the LNP surface against the chemical reactions promoted by the electrolyte oxidation at a high potential, the subsurface LNP will be involved in the charge transfer across the interface. It has been revealed that higher annealing temperatures are favorable for the formation of the SEI, which is stable under a high potential. These investigations show clearly that the SEI layer plays an important role in the stability of the cathode materials under a high operation potential. Additional work on the preparation of redox active LNP by increasing its electronic conductivity and, simultaneously, the design of surface conditions enabling the formation of highly protective SEI layer on the LNP surface is in the progress.

Summary

Quasi in-situ SPES and XANES experiments on the $LiNiPO_4$ - liquid electrolyte interface vs applied charging potential have demonstrated that carbon-free $LiNiPO_4$ films are chemically compatible with $LiPF_6$/DMC/FEC/0.2%-TMB electrolyte. By immersion of the cathode material to the electrolyte, no chemical reactions causing the change of the oxidation state of Ni ions at the interface or charge transfer to the lattice oxygen site are observed, independendly of the

annealing temperature of the $LiNiPO_4$ films during their preparation. However, we clearly demonstrated that the stability of the interface at a high charging potential depends strongly on the preparation conditions of $LiNiPO_4$. The $LiNiPO_4$ films grown at higher temperatures (∼740°C) form more stable SEI, where no decomposition of the $LiNiPO_4$ surface occurs up to 5.2 V. This work is a first step towards the design and preparation of stable and redox active olivine-$LiNiPO_4$ thin film cathode material.

Acknowledgments

This work was supported by the German Science Foundation (DFG, CH 566/2-1). The authors thank the Helmholtz Zentrum Berlin (BESSY II) and Elettra Sincrotrone Trieste SCpA (Italy) for the allocation of synchrotron radiation beamtime at the SoLiAS endstation at the U56 II/PGM-1 beamline and the CNR endstation BACH, respectively. S. N. and E. M. acknowledge the national grant Futuro in Ricerca 2012 RBFR128BEC and Progetto Premiale 2012 ABNANOTECH. We are thankful also to Dr. Federica Bondino and Dr. Igor Pís for the technical support at BACH beamline. G. C. greatly appreciates Prof. Doron Aurbach for the suggestion of the electrolytes suitable for olivine materials.

ORCID

Gennady Cherkashinin https://orcid.org/0000-0001-8363-6028
Mikhail V. Lebedev https://orcid.org/0000-0002-0249-5161

References

1. R. Hausbrand, G. Cherkashinin, H. Ehrenberg, M. Gröting, K. Albe, C. Hess, and W. Jaegermann, *Mater. Science Engineer. B*, **192**, 3 (2015).
2. G. G. Eshetu, M. Armand, B. Scrosati, and S. Passerini, *Angew. Chem. Int. Ed.*, **53**, 13342 (2014).
3. J. Li, C. Ma, M. Chi, C. Liang, and N. J. Dudney, *Adv. Energy Mat.*, **5**, 1401408 (2015).
4. J. B. Goodenough and Y. Kim, *Chem. Mat.*, **22**, 587 (2010).
5. G. Cherkashinin, S. U. Sharath, and W. Jaegermann, *Adv. Energy Mater.*, **7**, 1602321 (2017).
6. G. Cherkashinin, D. Ensling, and W. Jaegermann, *J. Mater. Chem. A*, **2**, 3571 (2014).
7. S. O. Kucheyev, C. Bostedt, T. van Buuren, T. M. Willey, T. A. Land, L. J. Terminello, T. E. Felter, A. V. Hamza, S. G. Demos, and A. J. Nelson, *Phys. Rev. B*, **70**, 245106 (2004).
8. A. Augustsson, G. V. Zhuang, S. M. Butorin, J. M. Osorio-Guillén, C. L. Dong, R. Ahuja, C. L. Chang, P. N. Ross, J. Nordgren, and J.-H. Guo, *J. Chem. Phys.*, **123**, 184717 (2005).
9. L. F. J. Piper, N. F. Quackenbush, S. Sallis, D. O. Scanlon, G. W. Watson, K.-W. Nam, X.-Q. Yang, K. E. Smith, F. Omenya, N. A. Chernova, and M. S. Whittingham, *J. Phys. Chem. C*, **117**, 10383 (2013).
10. H. M. Hollmark, T. Gustafsson, K. Edström, and L.-C. Duda, *Phys. Chem. Chem. Phys.*, **13**, 20215 (2011).
11. R. Hausbrand, G. Cherkashinin, M. Fingerle, and W. Jaegermann, *J. Electron Spectr. Relat. Phenom.*, **221**, 65 (2017).
12. J. N. Chen and J. W. Rabalais, *Surf. Sc.*, **176**, L879 (1986).
13. G. Cherkashinin, M. Motzko, N. Schulz, T. Späth, and W. Jaegermann, *Chem. Mater.*, **27**, 2875 (2015).
14. G. Cherkashinin and W. Jaegermann, *J. Chem. Phys.*, **144**, 184706 (2016).
15. E. Markevich, K. Fridman, R. Sharabi, R. Elazari, G. Salitra, H. E. Gottlieb, G. Gershinsky, A. Garsuch, G. Semrau, M. A. Schmidt, and D. Aurbach, *J. Electrochem. Soc.*, **160**, A1824 (2013).
16. M. Nie, J. Demeaux, B. T. Young, D. R. Heskett, Y. Chen, A. Bose, J. C. Woicik, and B. L. Lucht, *J. Electrochem. Soc.*, **162**, A7008 (2015).
17. E. Markevich, G. Salitra, and D. Aurbach, *ACS Energy Lett.*, **2**, 1337 (2017).
18. V. Etacheri, O. Haik, Y. Goffer, G. A. Roberts, I. C. Stefan, R. Fasching, and D. Aurbach, *Langmuir*, **28**, 965 (2011).
19. H. Nakai, T. Kubota, A. Kita, and A. Kawashima, *J. Electrochem. Soc.*, **158**, A798 (2011).
20. J. Wolfenstine and J. Allen, *J. Power Sourc.*, **142**, 389 (2005).
21. A. Örnek, *Chem. Engineer. J.*, **331**, 501 (2018).
22. A. Örnek, *J. Colloid Interf. Sci.*, **504**, 468 (2017).
23. G. Cherkashinin, K. Nikolowski, H. Ehrenberg, S. Jacke, L. Dimesso, and W. Jaegermann, *Phys. Chem. Chem. Phys.*, **14**, 12321 (2012).
24. S.-W. Cho and K.-S. Ryu, *Mater. Chem. Phys.*, **135**, 533 (2012).
25. A. Mauger, C. M. Julien, M. Armand, J. B. Goodenough, and K. Zaghib, *Current Opinion Electrochem.*, **6**, 63 (2017).